AD-A084 748 COLORADO UNIV AT BOULDER ELECTROMAGNETICS LAB F/G 20/6
A HYBRID METHOD FOR PARAXIAL BEAM PROPAGATION IN MULTIMODE OPTI--ETC(U)
JAN 80 D C CHANG, E F KUESTER DAAG29-78-G-0173
UNCLASSIFIED SCIENTIFIC-54 ARO -15632.3-EL NL

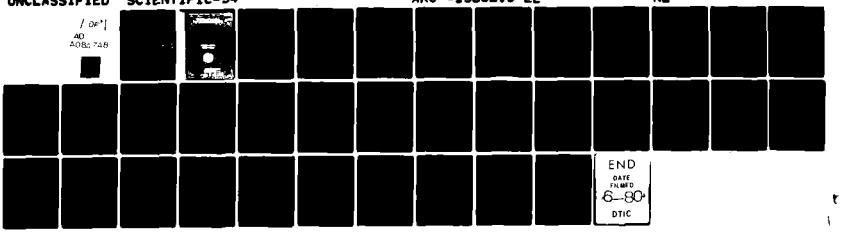

UNCLASSIFIED
SECURITY CLASSIFICATION OF THIS PAGE (When Data Entered)

REPORT DOCUMENTATION PAGE

READ INSTRUCTIONS BEFORE COMPLETING FORM

1. REPORT NUMBER: (19) 15632.3-EL	2. GOVT ACCESSION NO.: AD A084748
3. RECIPIENT'S CATALOG NUMBER	
4. TITLE (and Subtitle): A HYBRID METHOD FOR PARAXIAL BEAM PROPAGATION IN MULTIMODE OPTICAL WAVEGUIDES	5. TYPE OF REPORT & PERIOD COVERED: (9) Technical rept.
	6. PERFORMING ORG. REPORT NUMBER
7. AUTHOR(s): (10) David C. Chang, Edward F. Kuester	8. CONTRACT OR GRANT NUMBER(s): (15) DAAG29-78-G-0173
9. PERFORMING ORGANIZATION NAME AND ADDRESS: University of Colorado, Department of Electrical Engineering, Boulder, CO 80309	10. PROGRAM ELEMENT, PROJECT, TASK AREA & WORK UNIT NUMBERS
11. CONTROLLING OFFICE NAME AND ADDRESS: U. S. Army Research Office, Post Office Box 12211, Research Triangle Park, NC 27709	12. REPORT DATE: Jan 80
	13. NUMBER OF PAGES: 32
14. MONITORING AGENCY NAME & ADDRESS (if different from Controlling Office): (18) ARO	15. SECURITY CLASS. (of this report): Unclassified
	15a. DECLASSIFICATION/DOWNGRADING SCHEDULE

16. DISTRIBUTION STATEMENT (of this Report)

Approved for public release; distribution unlimited.

(12) 36

17. DISTRIBUTION STATEMENT (of the abstract entered in Block 20, if different from Report)

NA

(14) SCIENTIFIC-54

18. SUPPLEMENTARY NOTES

The view, opinions, and/or findings contained in this report are those of the author(s) and should not be construed as an official Department of the Army position, policy, or decision, unless so designated by other documentation.

19. KEY WORDS (Continue on reverse side if necessary and identify by block number)

optical waveguides
computation
wave propagation
paraxial beams
field computations
multimode waveguides

20. ABSTRACT (Continue on reverse side if necessary and identify by block number)

A hybrid (non-ray, non-modal) method for computing the fields of a paraxial beam propagating in a multimode waveguide (parallel-plate or dielectric slab) at large axial distances is presented. The method is based on the Fourier and Fresnel self-imaging properties of these waveguides, and is capable of high accuracy. The method is much more efficient than ray or mode approaches, while giving complete field information which coupled-power equations do not provide.

DD FORM 1 JAN 73 1473 EDITION OF 1 NOV 65 IS OBSOLETE

UNCLASSIFIED
SECURITY CLASSIFICATION OF THIS PAGE (When Data Entered)

409119

Scientific Report No. 54

A HYBRID METHOD FOR PARAXIAL BEAM PROPAGATION IN MULTIMODE OPTICAL WAVEGUIDES

by

David C. Chang and Edward F. Kuester

January 1980

Electromagnetics Laboratory
Department of Electrical Engineering
University of Colorado
Boulder, Colorado 80309

This research was supported by Army Research Office (ARO) under grant DAAG29-G-0173, monitored by Dr. J. Mink.

A HYBRID METHOD FOR PARAXIAL BEAM PROPAGATION IN MULTIMODE OPTICAL WAVEGUIDES

by

David C. Chang and Edward F. Kuester

Electromagnetics Laboratory
Department of Electrical Engineering
University of Colorado
Boulder, Colorado 80309

Abstract

A hybrid (non-ray, non-modal) method for computing the fields of a paraxial beam propagating in a multimode waveguide (parallel-plate or dielectric slab) at large axial distances is presented. The method is based on the Fourier and Fresnel self-imaging properties of these waveguides, and is capable of high accuracy. The method is much more efficient than ray or mode approaches, while giving complete field information which coupled-power equations do not provide.

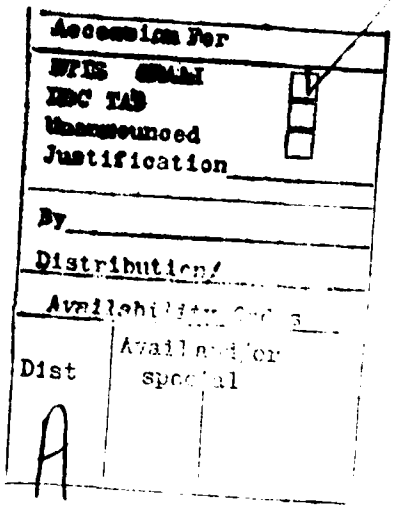

I. INTRODUCTION

Multimode optical fibers appear at present to be the most common optical waveguiding medium for applications in the immediate future. Incoherent sources and relatively simple detectors can be used, and the tolerance problems encountered with single-mode fibers are far less severe with such waveguides.

At present, there are essentially three methods available for field computation in multimode waveguides. First, one can take a pure modal approach--the excitation amplitude of each mode is computed, and all modes are summed together. Although in principle exact, this approach suffers not only from the large number of modes which must be kept track of ($100 \sim 1000$ for a typical fiber; $30 \sim 100$ for a slab geometry) but also from a large degree of cancellation of terms in the mode sum when the field does not match that of an individual mode. Examples of the application of this method may be found in [1]. Although in some special cases approximate closed-form results are available, a computer analysis is generally required, and roundoff errors can be expected to accumulate, especially for large propagation distances.

A second approach is that of geometrical optics (sometimes encountered as the WKB method). An excellent discussion of this approach has been given by Gloge and Marcatili [2] (see also [3]). Here one approximates the effect of a large number of discrete propagating modes by a continuously distributed propagation constant belonging to a "continuous spectrum" of modes. These, when computed under the WKB approximation, can be interpreted as a cone of rays lying within some characteristic acceptance

angle of the fiber. The propagation problem then reduces to that of determining the amplitude with which each ray is excited, and tracing it down the length of the guide. Intuitively more suitable for multimode guides because of the "high-frequency" nature of the problem, this approach is nonetheless approximate by virtue of the geometrical optics technique. Moreover, in a situation where paraxial propagation conditions exist (see below), a large number of rays can be expected to contribute at large propagation distances (hundreds of meters or several kilometers may not be uncommon). In this region, the geometrical optics approach can be seen to suffer from similar disadvantages as does the first.

A third approach (see, e.g., [4],[5]) is a purely numerical one, wherein the partial differential equation--Helmholtz or its parabolic approximant--is tackled directly, without the use of either mode or ray concepts. In [4] and [5], the equation is discretized and solved with the aid of fast Fourier transform techniques. This method, like the first, is also capable of arbitrary accuracy in principle, and requires neither a detailed knowledge of a large number of modes, nor the tracing of a large number of ray paths. Again, however, when very long propagation distances are being studied, the discretization of the wave equation in the longitudinal direction can lead to large error accumulations which do not seem easily avoidable by this technique.

Finally, we might also mention here the coupled-power equations approach [1]. This method seeks only to find the total power carried by each mode, since for many applications the details of the field distribution from each mode are not of interest. One then takes a statistical approach to these equations, and obtains useful results for pulse dispersion

when each mode of the guide is detectable only through its total power. There are many other applications, however, when the fields themselves are important, such as in the design of couplers, splitters, switches, splicers, etc., and it is this problem in which we are interested here.

The method we propose is based on the imaging properties of multimode waveguides. In the paraxial approximation, a parallel-plate or dielectric slab waveguide will periodically reconstruct the field pattern at the input plane (and, at more frequent intervals, a string of such replicas). Because of this, we need only perform our field computations within the space of one of these periods, and will not suffer the loss of accuracy at large distances associated with the methods described above. Our computations will be performed for a parallel-plate waveguide with perfectly conducting walls, but the results are immediately applicable to the dielectric slab waveguide (Appendix A). The method will allow a simple formula to be obtained for the propagation of a Gaussian beam of substantially narrower width than that of the guide. (Note that the study by Felsen and Shin [6] of beam propagation in waveguides is in practice restricted to beams which propagate obliquely to the axis of the guide, and actually will suffer from the same drawbacks at large axial distances as does the ray method, although it is probably superior to the ray method at shorter distances). Numerical comparisons with exact (modal) calculations are quite favorable, even for rather large propagation distances.

II. THE PARAXIAL APPROXIMATION

To fix ideas, let us consider the parallel-plate waveguide illustrated in Fig. 1 (the discussion of this section, however, is quite general and need not be restricted to this specific waveguide). The walls at $x = 0$ and $x = a$ are perfectly conducting, and some known source produces a given excitation or input field at the plane $z = 0$. For simplicity, we restrict ourselves to two dimensional, TE fields, so that the entire field $\bar{H} = \bar{a}_x H_x + \bar{a}_z H_z$, $\bar{E} = \bar{a}_y E_y$, where $\bar{a}_x, \bar{a}_y, \bar{a}_z$ are Cartesian unit vectors, can be derived from the scalar function E_y which satisfies

$$\left(\frac{\partial^2}{\partial x^2} + \frac{\partial^2}{\partial z^2} + k^2\right) E_y = 0 \tag{1}$$

for $z > 0$. Here $k = \omega\sqrt{\mu\varepsilon}$, where a time dependence $\exp(i\omega t)$ has been assumed, and μ, ε are the electrical parameters of the medium filling the waveguide.

In the paraxial approximation, we write

$$E_y(x,z) = e^{-ikz} A(x,z) \tag{2}$$

and assume that most propagation takes place nearly in the z-direction; that is, $A(x,z)$ as a function of z varies slowly compared to $\exp(-ikz)$. Inserting (2) into (1) we obtain

$$\left(\frac{\partial^2}{\partial x^2} - 2ik\frac{\partial}{\partial z} + \frac{\partial^2}{\partial z^2}\right) A(x,z) = 0 \tag{3}$$

and in the paraxial approximation, we neglect the $\partial^2/\partial z^2$ term compared to the first derivative term because of the slow variation of $A(x,z)$ in z assumed above. We thus obtain the following parabolic equation for $A(x,z)$[7]:

$$\left(\frac{\partial^2}{\partial x^2} - 2ik\,\frac{\partial}{\partial z}\right) A(x,z) = 0 \tag{4}$$

To put this approximation on a more quantitative footing, we can apply some ideas from the boundary-layer technique [8]. By "stretching" the variable x into a new variable $\nu = x/a$, we can deal with a transverse variable ν which is O(1) over the entire cross-section of the guide. When rewritten in terms of ν, equation (4) becomes

$$\left(\frac{\partial^2}{\partial \nu^2} - 2ika^2\,\frac{\partial}{\partial z}\right) A(\nu,z) = 0 \tag{5}$$

which suggests that the scaling $\zeta = \text{const}\ z/ka^2$ might be convenient. For reasons which will become clear in the next section, we choose $\zeta = \pi z/4ka^2$. Making both changes of variable in (3), we have

$$\left(\frac{\partial^2}{\partial \nu^2} - \frac{\pi i}{2}\,\frac{\partial}{\partial \zeta}\right) A(\nu,\zeta) = -\frac{\pi^2}{16k^2a^2}\,\frac{\partial^2 A(\nu,\zeta)}{\partial \zeta^2} \tag{6}$$

It is natural now to assume a solution to (6) of the form

$$A(\nu,\zeta) \sim A_0(\nu,\zeta) + \frac{1}{k^2a^2}\,A_1(\nu,\zeta) + \frac{1}{k^4a^4}\,A_2(\nu,\zeta) + \cdots \tag{7}$$

so that, by matching powers of $(ka)^{-2}$, we find a recurrent set of equations for A_0, A_1, etc.:

$$\left(\frac{\partial^2}{\partial \nu^2} - \frac{\pi i}{2}\,\frac{\partial}{\partial \zeta}\right) A_0(\nu,\zeta) = 0 \tag{8}$$

$$\left(\frac{\partial^2}{\partial \nu^2} - \frac{\pi i}{2}\,\frac{\partial}{\partial \zeta}\right) A_1(\nu,\zeta) = -\frac{\pi^2}{16}\,\frac{\partial^2 A_0(\nu,\zeta)}{\partial \zeta^2} \tag{9}$$

and so on. As initial conditions at $\zeta = 0$, we require $A_0(x/a,0) = E_y(x,0)$--a given function--while $A_1(\nu,0) = A_2(\nu,0) = \ldots = 0$.

We are now in a position to estimate the magnitude of the correction term A_1, and therefore the error involved in the paraxial approximation. It is easily verified that, for example,

$$A_1(\nu,\zeta) = \frac{i\zeta}{2\pi} \frac{\partial^4 A_0(\nu,\zeta)}{\partial \nu^4} = -\frac{i\pi\zeta}{8} \frac{\partial^2 A_0(\nu,\zeta)}{\partial \zeta^2} \tag{10}$$

with A_2, A_3, etc., given by similar expressions. Because of the scaling of the variables ν and ζ, the differentiations in (10) do not increase the order of magnitude of the function A_0. Thus if A_0 is $O(1)$, then

$$|A_1(\nu,\zeta)| \lesssim O(\zeta) \tag{11}$$

so a criterion for the accuracy of the paraxial approximation $(A \simeq A_0)$ is that $\zeta/k^2a^2 \ll 1$, or in other words,

$$kz \ll (ka)^4 \tag{12}$$

In addition, of course, we also have the condition $k^2a^2 \gg 1$, which is implicit in the expansion (7) and the fact that the guide is highly multimode.

These arguments are not restricted to the case of a parallel-plate waveguide. However, as with any "order-of-magnitude" arguments, they say nothing about the proportionality constant implicit in (11). In fact, this constant will depend sensitively on the function $A_0(\nu,\zeta)$, mostly through its initial value $A_0(\nu,0)$. Thus, a detailed study of the estimate (11) should be made when using the paraxial approximation in any specific situation. This procedure is discussed in some detail by Tappert [9], who also gives a large number of references to its use in acoustics. In Appendix A, we consider the paraxial approximation for

a dielectric slab waveguide, and demonstrate an approximate equivalence with a parallel-plate waveguide.

In closing, we might also note that Polyanskii [11] has obtained a formula relating the solution of the parabolic equation to that of the Helmholtz equation which is an alternative to the perturbation series (7). Further, another variant of the parabolic equation more suitable for off-axis propagation has been proposed in [12].

III. GREEN'S FUNCTION AND IMAGING

By well-known techniques, the field $E_y(x,z)$ for $z>0$ in the waveguide can be expressed in terms of the field $E_y(x,0)$ at an input plane ($z=0$) by means of a Green's function $G(x,x';z)$:

$$E_y(x,z) = \int_0^a E_y(x',0)G(x,x';z)dx' \tag{13}$$

where G can be expressed as a modal expansion:

$$G(x,x';z) = \frac{2}{a}\sum_{m=1}^{\infty} \sin\frac{m\pi x}{a}\sin\frac{m\pi x'}{a}e^{-i\beta_m z};\ z \geq 0 \tag{14}$$

where $\beta_m = (k^2 - m^2\pi^2/a^2)^{\frac{1}{2}}$. On the other hand, the Green's function G_o for the paraxial approximation (2), (4) to E_y is given by:

$$G_o(x,x';z) = \frac{2}{a}e^{-ikz}\sum_{m=1}^{\infty} \sin\frac{m\pi x}{a}\sin\frac{m\pi x'}{a}e^{jzm^2\pi^2/2ka^2} \tag{15}$$

Evidently G_o could have been obtained from G by replacing β_m by the first two terms of its binomial expansion $\beta_m \simeq k - m^2\pi^2/2ka^2$. We see that whereas G has a large but finite number of modes which propagate, the paraxial approximation G_o has infinitely many such modes. It is convenient to rewrite G_o by expressing the sine functions as exponentials; the result is:

$$G_o(x,x';z) = \frac{1}{2a}e^{-ikz}\sum_{m=-\infty}^{\infty} e^{jzm^2\pi^2/2ka^2}\left\{e^{-im\pi(x-x')/a} - e^{-im\pi(x+x')/a}\right\} \tag{16}$$

If we define

$$z_{11} = 4ka^2/\pi \tag{17}$$

(so that the stretched variable of the previous section is $\zeta = z/z_{11}$), then

$$G_0(x,x';z) = \frac{1}{2a} e^{-ikz} \sum_{m=-\infty}^{\infty} e^{2\pi i m^2 z/z_{11}} \left\{ e^{-im\pi(x-x')/a} - e^{-im\pi(x+x')/a} \right\} \quad (18)$$

Equation (18) is the basis for the so-called Fourier-and Fresnel-imaging properties of this waveguide [13]. It is easily seen from (18) that $\exp(ikz)G_0$ is a periodic function of z:

$$G_0(x,x';z + z_{11}) = G_0(x,x';z)e^{-ikz_{11}} \quad (19)$$

In particular, since (13) implies that $G(x,x';0)$ is equal to $\delta(x-x')$ for $0 \leq (x,x') \leq a$, we have

$$G_0(x,x'; nz_{11}) = \delta(x-x')e^{-iknz_{11}} \quad (20)$$

for any integer n, i.e., the input plane field is replicated at each of the Fourier image planes $z = nz_{11}$. This phenomenon was first investigated theoretically for unbounded periodic gratings, and the imaging distance was first given by Rayleigh [14]. Later treatments have been given in [13], [15]-[17]. Because of the mathematical equivalence of a waveguide with a periodic system, this imaging also occurs in waveguides--a fact apparently first noticed by Rivlin and Shul'dyaev [18] and discussed at length by a number of authors [10],[19]-[23].

An even more interesting occurrence shows up at $z = z_{pq}$, where

$$z_{pq} = \frac{q}{p} z_{11} \quad (21)$$

and p and q are some positive integers. Let us consider the sum

$$Q_{pq}(x) = \sum_{m=-\infty}^{\infty} e^{-im\pi x/a + 2\pi i m^2 z_{pq}/z_{11}} \quad (22)$$

Let $m = p\ell + r$, where r runs from 0 to p-1, and express (22) as a double sum:

$$Q_{pq}(x) = \sum_{\ell=-\infty}^{\infty} \sum_{r=0}^{p-1} e^{-i\pi x(p\ell+r)/a + 2\pi i q[p\ell^2+2\ell r + r^2/p]}$$

$$= \sum_{r=0}^{p-1} e^{-i\pi rx/a + 2\pi i q r^2/p} \left(\sum_{\ell=-\infty}^{\infty} e^{-i\pi p\ell x/a} \right) \tag{23}$$

However, the summation in parenthesis is nothing more than $Q_{11}(px)$, although now the argument can range not just from -a to +a (or 0 to 2a), but from -pa to +pa (or 0 to 2pa). Making use of the formula [24]:

$$\sum_{m=-\infty}^{\infty} e^{2\pi i m x/d} = d \sum_{n=-\infty}^{\infty} \delta(x-nd) \tag{24}$$

for any positive d,

$$Q_{pq}(x) = \frac{2a}{p} \sum_{r=0}^{p-1} e^{-i\pi rx/a + 2\pi i q r^2/p} \sum_{n=-\infty}^{\infty} \delta(x - \frac{2na}{p}) \tag{25}$$

From (18), then, we have

$$G_o(x,x';z_{pq}) = e^{-ikz_{pq}} \sum_{n=-\infty}^{\infty} c_n(p,q)[\delta(x-x' - \frac{2na}{p}) - \delta(x+x' - \frac{2na}{p})] \tag{26}$$

where the coefficients c_n are given by

$$c_n(p,q) = \frac{1}{p} \sum_{r=0}^{p-1} e^{2\pi i r(rq+n)/p} \tag{27}$$

For p = 1, only one of the delta-functions, $\delta(x-x')$, is nonzero in the range $0 \leq (x,x') \leq a$, and we recover the single Fourier image described before. If $p > 1$ on the other hand, more of the delta-functions in (26) may appear in this range. Each one contributes to (13) a replica of the input field which is <u>shifted</u> by some amount in the x-direction,

and whose amplitude is $|c_n(p,q)|$ times that of the original image. Any terms arising from the terms $\delta(x + x' - 2na/p)$ are inverted as well. Images of this type have been called Fresnel images.

For an input function not symmetric with respect to the center of the guide $x = a/2$, we have depicted the various images along with their (complex) amplitudes in Fig. 2 for z_{21}, z_{31} and z_{41}. The phase factor $\exp(-ikz)$ is omitted in this figure. Figure 2(a) illustrates the input function $E_y(x,0)$. At $z = z_{21}$, there is only one image, which is inverted with respect to the original, but is also a further 180° out of phase with respect to the input after the factor $\exp(-ikz)$ is accounted for (Fig. 2(b)). At $z = z_{31}$ (Fig. 2(c)), the situation is more involved. One of the images is an unchanged replica, reduced in amplitude by $1/\sqrt{3}$ and phase shifted by 90°. The other two image terms have "broken up" and rearranged the original pattern. Between them, they both contain two complete replicas of the original, and again the amplitude of each is reduced by $1/\sqrt{3}$. Note that this amplitude reduction is consistent with the fact that all of the power of the original pattern must be divided between the three split images. At $z = z_{41}$, there is both an erect and an inverted image (Fig. 2(d)).

For the special case of a symmetric excitation, $E_y(x,0) = E_y(a - x,0)$, z_{21}, z_{41} and indeed z_{81} all reproduce the original input function (Fig.3(a)). If the input function is a beam of sufficiently narrow width, we can recognize three essentially distinct images at z_{31} (Fig. 3(b)). At other image planes, similar conclusions hold.

The Fourier and Fresnel images allow us, in principle, to compute the field in the waveguide at any point z_{pq} (and any arbitrary value of z can be approached as nearly as desired by such a point). This

procedure could, however, require a large value of p, and hence an inordinately large number of image terms, resulting in a method which is no more efficient than the modal approach. In the next section, we will show how, for a certain specific type of excitation, efficient field computation can be carried out for any value of z, using only a relatively small number of images.

Let us emphasize in closing this section that the imaging phenomenon results from the collective interference of the mode sum (14), or alternatively from the interference of the series of "rays" (plane waves) represented by (18), depending on one's preferred physical picture. The only assumption involved is the paraxial approximation, and in the case of the parallel-plate waveguide, no approximation of the mode functions themselves is needed. In the case of a dielectric waveguide, some small higher-order corrections to the mode functions will be needed (see Appendix A).

IV. PROPAGATION OF A GAUSSIAN BEAM

Consider the initial field distribution

$$E_y(x,0) = e^{-(x-x_0)^2/2w_0^2} \tag{28}$$

i.e., a Gaussian beam centered at x_0 with waist parameter w_0. Let $0 < x_0 < a$, and assume that the "tails" of the beam are negligible at the walls of the guide:

$$w_0 << x_0 \; ; \qquad w_0 << a - x_0$$

In addition, we also suppose that the beam is well collimated, $kw_0 >> 1$. Under these conditions and the paraxial approximation, (13) can be replaced by

$$E_y(x,z) = \int_{-\infty}^{\infty} e^{-(x'-x_0)^2/2w_0^2} \, G_0(x,x';z)dx' \tag{29}$$

We wish to evaluate (29) for arbitrary (not necessarily rational) values of z/z_{11}.

To do this it is convenient to express G_0 in terms of the Jacobian theta-function ϑ_3, defined by Whittaker and Watson [25] as:

$$\vartheta_3(z|\tau) = \sum_{m=-\infty}^{\infty} e^{m^2\pi i\tau + 2miz} \tag{30}$$

(the argument z is conventionally used in this connection and should not be confused with the cartesian coordinate z used above). This function has a wealth of useful properties which we summarize in Appendix B. The theta-function appears in solutions of other parabolic equations, such as the heat equation [28]. In the paraxial parabolic equation, however, the arguments z and τ are both real (see below) and ϑ_3 must be treated as a generalized function.

Using (30), G_o becomes

$$G_o(x,x';z) = \frac{1}{2a} e^{-ikz} \left\{ \vartheta_3\left(\frac{\pi(x-x')}{2a} \middle| \frac{2z}{z_{11}}\right) - \vartheta_3\left(\frac{\pi(x+x')}{2a} \middle| \frac{2z}{z_{11}}\right) \right\} \tag{31}$$

From (29), then

$$E_y(x,z) = \frac{e^{-ikz}}{2a} \int_{-\infty}^{\infty} e^{-(x'-x_o)^2/2w_o^2} \left[\vartheta_3\left(\frac{\pi(x-x')}{2a} \middle| \frac{2z}{z_{11}}\right) - \vartheta_3\left(\frac{\pi(x+x')}{2a} \middle| \frac{2z}{z_{11}}\right)\right] dx' \tag{32}$$

With the help of (B.11) we obtain

$$E_y(x,z) = \frac{w_o}{a}\sqrt{\frac{\pi}{2}}\, e^{-ikz} \left\{ \vartheta_3\left(\frac{\pi(x-x_o)}{2a} \middle| \frac{2z}{z_{11}} + \frac{i\pi w_o^2}{2a^2}\right) - \vartheta_3\left(\frac{\pi(x+x_o)}{2a} \middle| \frac{2z}{z_{11}} + \frac{i\pi w_o^2}{2a^2}\right)\right\} \tag{33}$$

Let us first consider the focussing relative to z_{11}. Let $z = qz_{11} + \Delta z$, where $-z_{11}/2 \le \Delta z \le z_{11}/2$ and q is an integer. From (B.3) and (B.8), we have

$$E_y(x,z) = \frac{w_o}{f(\Delta z)} e^{-ikz} \left\{ e^{-(x-x_o)^2/2f^2(\Delta z)} \vartheta_3\left(\frac{ia(x-x_o)}{f^2(\Delta z)} \middle| \frac{2ia^2}{\pi f^2(\Delta z)}\right) \right. \tag{34}$$

$$\left. - e^{-(x+x_o)^2/2f^2(\Delta z)} \vartheta_3\left(\frac{ia(x+x_o)}{f^2(\Delta z)} \middle| \frac{2ia^2}{\pi f^2(\Delta z)}\right)\right\}$$

where we have defined a "complex waist parameter" $f(\Delta z)$ as

$$f^2(\Delta z) = w_o^2\left[1 - i\,\frac{4a^2}{\pi w_o^2}\,\frac{\Delta z}{z_{11}}\right] = w_o^2 - i\Delta z/k \tag{35}$$

Using (B.12), we can further reduce (34) to

$$E_y(x,z) = \frac{w_o}{f(\Delta z)} e^{-ikz} \sum_{m=-\infty}^{\infty} \left\{ e^{-(x-x_o+2ma)^2/2f^2(\Delta z)} - e^{-(x+x_o+2ma)^2/2f^2(\Delta z)} \right\} \tag{36}$$

Now

$$\frac{1}{2f^2(\Delta z)} = \frac{1}{2w^2(\Delta z)} + \frac{i\Delta z/kw_o^2}{2w^2(\Delta z)} \tag{37}$$

where the waist size $w(\Delta z)$ is given by

$$w^2(\Delta z) = w_o^2 + (\Delta z/kw_o)^2 \tag{38}$$

so we can see that (36) represents an infinite series of Gaussian beams, each broadened from its focal plane $z = qz_{11}$ as if it were propagating in free space. We illustrate this in Fig. 4. As Δz increases, more and more of the "image" beams contribute significantly to the field in $0 \leq x \leq a$. At $\Delta z = z_{11}/2$ (say), the waist size has become

$$w^2(z_{11}/2) = w_o^2 + (2a^2/\pi w_o)^2 \simeq 4a^4/\pi^2 w_o^2 >> a^2$$

because our assumptions about the beam imply $a >> w_o$. Thus we may require quite a few terms of the image series (36) in order to compute the fields at certain values of z.

For such values of Δz, we seek to improve the efficiency of our scheme by transforming (33) in a somewhat different manner. Applying relation (B.9), we find that

$$E_y(x,z) = \frac{w_o}{a}\sqrt{\frac{\pi}{2}}\, e^{-ikz} \sum_{r=0}^{p-1} e^{\pi i r^2 2z/z_{11} - \pi^2 r^2 w_o^2/2a^2}$$
$$\cdot \left\{ e^{i\pi r(x-x_o)/a}\, \vartheta_3\left(p\left[\frac{\pi(x-x_o)}{2a} + \frac{2\pi rz}{z_{11}} + ir\,\frac{\pi^2 w_o^2}{2a^2}\right] \middle| p^2\,\frac{2z}{z_{11}} + ip^2\,\frac{\pi w_o^2}{2a^2}\right)\right.$$
$$\left. - e^{i\pi r(x-x_o)/a}\, \vartheta_3\left(p\left[\frac{\pi(x+x_o)}{2a} + \frac{2\pi rz}{z_{11}} + ir\,\frac{\pi^2 w_o^2}{2a^2}\right] \middle| p^2\,\frac{2z}{z_{11}} + ip^2\,\frac{\pi w_o^2}{2a^2}\right)\right\} \tag{39}$$

for any specified positive integer p. Now, let $z = z_{pq} + \Delta z_p$, where now $-z_{11}/2p \le \Delta z_p \le z_{11}/2p$. The periodicity properties (B.3) and (B.4) allow us to replace z by Δz_p in the arguments of the theta-functions in (39). Subsequently applying (B.8) results in

$$E_y(x,z) = \frac{w_o}{pf(\Delta z_p)} e^{-ikz} \sum_{r=0}^{p-1} e^{2\pi i r^2 q/p} \left\{ e^{-(x-x_o)^2/2f^2(\Delta z_p)} \vartheta_3\left(\frac{ia(x-x_o)}{pf^2(\Delta z_p)} - \frac{\pi r}{p} \middle| \frac{2ia^2}{\pi p^2 f^2(\Delta z_p)} \right) - e^{-(x+x_o)^2/2f^2(\Delta z_p)} \vartheta_3\left(\frac{ia(x+x_o)}{pf^2(\Delta z_p)} - \frac{\pi r}{p} \middle| \frac{2ia^2}{\pi p^2 f^2(\Delta z_p)} \right) \right\} \tag{40}$$

where f is defined in (35) as before. For $p = 1$, this reduces to (34) as expected. Finally, through the use of (B.12) we obtain

$$E_y(x,z) = \frac{w_o}{f(\Delta z_p)} e^{-ikz} \frac{1}{p} \sum_{r=0}^{p-1} e^{2\pi i r^2 q/p} \left\{ \sum_{m=-\infty}^{\infty} e^{-2\pi i m r/p} \left[e^{-(x-x_o+2ma/p)^2/2f^2(\Delta z_p)} - e^{-(x+x_o+2ma/p)^2/2f^2(\Delta z_p)} \right] \right\} \tag{41}$$

Clearly, equation (41) represents a string of Fresnel images at z_{pq}, broadened by their additional propagation distance Δz_p as evidenced by the factor $f(\Delta z_p)$ (compare (26)-(27)). A slight rearrangement of (41) yields a single summation (letting $m \to -n$):

$$E_y(x,z) = \frac{w_o}{f(\Delta z_p)} e^{-ikz} \sum_{n=-\infty}^{\infty} c_n(p,q) \left\{ e^{-(x-x_o-2na/p)^2/2f^2(\Delta z_p)} - e^{-(x+x_o-2na/p)^2/2f^2(\Delta z_p)} \right\} \tag{42}$$

where $c_n(p,q)$ is given by (27).

How, then, is p to be chosen? Our goal is to minimize the number of terms of the series (42) required to give a specified accuracy.

If we elect to truncate the series at $n = \pm N$ such that the terms at this point have magnitude less than, say, e^{-8}, N will be the next larger integer than

$$2pw(\Delta z_p)/a$$

where w is given by (38) and we have examined the "worst case" when $x = x_0$ in the first term of the summand in (42). As Δz_p varies from 0 to $z_{11}/2p$, this quantity varies from $2pw_0/a$ to

$$\frac{4}{\pi}\,\frac{a}{w_0}\left(1 + \frac{\pi^2 p^2 w_0^4}{4a^4}\right)^{\frac{1}{2}}$$

If $p < a/2w_0$, N will vary between a minimum of 1 and a maximum of about $4a/\pi w_0$. If, on the other hand, $p > 2a^2/\pi w_0^2$, then N is at least $4a/\pi w_0$ as a minimum, and at least $4/\sqrt{2}\,a/\pi w_0$ as a maximum. Clearly then, such large values of p are undesirable for efficient field computations (because more images of the Gaussian beam are fitted inside the waveguide than can be accommodated without severe overlap), and there is no apparent reason to let p exceed a value on the order of a/w_0. On the other hand, for a specific value of z, Δz_p may be much closer to zero for a smaller value of p, and in such cases the smaller choice of p might be desirable. However, a single choice of p for all values of z results in a simpler computer program, and it is seen from the foregoing discussion that a value of about a/w_0 is nearly optimal.

V. NUMERICAL RESULTS

Numerical results for $0 \leq z \leq z_{81}$ were computed for a symmetrical Gaussian beam

$$E_y(x,0) = e^{-(x-a/2)^2/2w_o^2}$$

for a waveguide with $ka = 973.4$, $kw_o = 110.3$. Computations were made using both an exact mode series (cf. (14)) and the hybrid-image representation (42). The two methods gave graphically indistinguishable results over this range, which are displayed in Fig. 5. Note that 5 or 6 is the maximum distinguishable number of beams in this case, and is a suitable choice for p.

Figure 6 shows that for very large values of z, the accuracy of the paraxial approximation has begun to deteriorate slightly. In a future paper, we will examine how to obtain closed-form expressions for this correction, but meanwhile we note that even for $z \simeq 250z_{11}$, the accuracy of the paraxial expression is quite good. If we take this example to model an optical waveguide with $a = 100\mu$, $w_o = 7.07\mu$, the distance $250z_{11}$ represents about a 50 m length of waveguide which of course is a huge number of wavelengths. We thus see that the paraxial approximation is capable of excellent accuracy over modest lengths of waveguide, even at optical frequencies.

VI. CONCLUSION

We have described a hybrid technique for computing the fields of a paraxial beam propagating in a multimode waveguide for very long distances. The method relies on the periodic Fourier and Fresnel imaging properties of the guide, and is highly efficient for beams of moderate width compared to either full modal or ray approaches. Numerical comparisons have confirmed the accuracy of this method.

This approach should be susceptible to generalizations in several directions. For a beam with oblique incidence (as in [6]), the parabolic approximation of section II can be modified when the dominant propagation factor in the z-direction is other than exp(-ikz) as indicated in [12]. Higher-order corrections to the paraxial solution for a dielectric slab similar to those for the metallic guide given in Section II can also be obtained. Slowly-varying guide widths and inhomogeneous refractive index profiles should also be tractable by similar methods. Investigations into these areas are currently being made, as is the generalization to waveguides of circular symmetry.

REFERENCES

[1] D. Marcuse, Theory of Dielectric Optical Waveguides. New York: Academic Press, 1974, ch. 1 and 5.

[2] D. Gloge and E.A.J. Marcatili, "Multimode theory of graded-core fibers," Bell Syst. Tech. J. vol. 52, pp. 1563-1578 (1973).

[3] H.-G. Unger, Planar Optical Waveguides and Fibers. Oxford: Clarendon Press, 1977, ch. 5.

[4] C. Yeh, L. Casperson and B. Szejn, "Propagation of truncated Gaussian beams in multimode fiber guides," J. Opt. Soc. Amer. vol. 68, pp. 989-993 (1978).

[5] M.D. Feit and J.A. Fleck, "Light propagation in graded-index optical fibers," Appl. Optics, vol. 17, pp. 3990-3998 (1978).

[6] L.B. Felsen and S.-Y. Shin, "Rays, beams, and modes pertaining to the excitation of dielectric waveguides," IEEE Trans. Micr. Theory Tech., vol. 23, pp. 150-161 (1975).

[7] J. A. Arnaud, Beam and Fiber Optics. New York: Academic Press, 1976, ch. 3.

[8] V.M. Babič and N.Y. Kirpičnikova, The Boundary-Layer Method in Diffraction Problems. Berlin: Springer-Verlag, 1979, ch. 5.

[9] F.D. Tappert, "The parabolic approximation method," in Wave Propagation and Underwater Acoustics (J.B. Keller and J.S. Papadakis, eds.). Berlin: Springer-Verlag, 1977, pp. 224-287.

[10] R. Ulrich, "Image formation by phase coincidences in optical waveguides," Opt. Commun. vol. 13, pp. 259-264 (1975).

[11] E.A. Polyanskii, "The connection between the solutions of the Helmholtz equation and those of Schrödinger type equations," Zh. Vychisl. Mat.Mat.Fiz. vol. 12, pp. 241-249 (1972) [in Russian; Engl. transl. in USSR Comp. Math. Math. Phys. vol. 12, no. 1, pp. 318-329 (1972)].

[12] P. Ya. Ufimtsev and G.D. Yakovleva, "Paraxial mode bunches in regular and irregular waveguides," Radiotekh. Elektron. vol. 22, pp. 451-465 (1977) [in Russian; Engl. transl. in Radio Eng. Electron. Phys. vol. 22, no. 3, pp. 16-28 (1977)].

[13] J.M. Cowley and A.F. Moodie, "Fourier Images: I,II,III," Proc.Phys. Soc. London, sec. B, vol. 70, pp. 486-496, 497-504, 505-513 (1957).

[14] Lord Rayleigh, "On copying diffraction-gratings, and on some phenomena connected therewith," Phil. Mag. ser. 5, vol. 11, pp. 196-205 (1881).

[15] J.T. Winthrop and C.R. Worthington, "Theory of Fresnel images. I. Plane periodic objects in monochromatic light," J. Opt. Soc. Amer. vol. 55, pp. 373-381 (1965).

[16] S. Blume, "Analogien zwischen elektrischen und wellenphysikalischen systemen," Optik, vol. 46, pp. 333-355 (1976).

[17] S. Blume, "Eine Raumfrequenzanalyse von Fourier- und Fresnelbildern," Optik, vol. 48, pp. 507-512 (1977).

[18] L.A. Rivlin and V.S. Shul'dyaev," Multimode waveguides for coherent light," Izv. VUZ Radiofizika vol. 11, pp. 572-578 (1968) [in Russian; Engl. transl. in Radiophys. Quantum Electron, vol. 11, pp. 318-321 (1968)].

[19] R. Ulrich and G. Ankele, "Self-imaging in homogeneous planar optical waveguides," Appl. Phys. Lett. vol. 27, pp. 337-339 (1975).

[20] R. Ulrich, "Light-propagation and imaging in planar optical waveguides," Nouv. Rev. Optique vol. 6, pp. 253-262 (1975).

[21] J.C. Campbell and T. Li, "Electro-optic multimode waveguide switch," Appl. Phys. Lett. vol. 33, pp. 710-712 (1978).

[22] R. Ulrich and T. Kamiya, "Resolution of self-images in planar optical waveguides," J. Opt. Soc. Amer. vol. 68, pp. 583-592 (1978).

[23] E.E. Grigor'eva and A.T. Semenov, "Waveguide image transmission in coherent light (review)," Kvant. Elektron. vol. 5, pp. 1877-1895 (1978) [in Russian; Engl. transl. in Sov.J. Quantum Electron. vol. 8, pp. 1063-1073 (1978)].

[24] M.J. Lighthill, Fourier Analysis and Generalised Functions. Cambridge: University Press, 1958, ch. 5.

[25] E.T. Whittaker and G.N. Watson, A Course of Modern Analysis. Cambridge: University Press, 1927, ch. 21.

[26] F. Tölke, Praktische Funktionenlehre, vol. 2, Berlin: Springer-Verlag, 1966, ch. 1.

[27] A. Krazer, Lehrbuch der Thetafunktionen. New York: Chelsea, 1970, pp. 65-69.

[28] E.T. Copson, Partial Differential Equations. Cambridge: University Press, 1975, pp. 262-265.

APPENDIX A

THE PARAXIAL APPROXIMATION FOR A DIELECTRIC SLAB

Consider the step-index dielectric slab waveguide shown in Fig. A.1. The slab has thickness b and refractive index n_0. The cladding index is n_1, and both media are assumed to be nonmagnetic. The TE modes for this waveguide have the field distribution [1]

$$E_y = \begin{cases} e^{-ik\alpha z} A\, e^{k\sqrt{\alpha^2-n_1^2}\,x} \sin\phi(\alpha) & x \le 0 \\ e^{-ik\alpha z} A \sin\left[k\sqrt{n_0^2-\alpha^2}\,x + \phi(\alpha)\right] & 0 \le x \le b \\ e^{-ik\alpha z} A \sin\left[k\sqrt{n_0^2-\alpha^2}\,b + \phi(\alpha)\right] e^{-k\sqrt{\alpha^2-n_1^2}(x-b)} & x \ge b \end{cases} \tag{A.1}$$

where A is an arbitrary constant amplitude. Here k is the wavenumber of free space, $k\alpha$ is the propagation constant of the mode, and $\phi(\alpha)$ is the phase shift associated with the Goos-Hänchen effect:

$$\phi(\alpha) = \sin^{-1}\left[kb\sqrt{n_0^2-\alpha^2}/V\right] \tag{A.2}$$

where V is the so-called normalized frequency :

$$V = kb\sqrt{n_0^2 - n_1^2} \tag{A.3}$$

Note that $V >> 1$ for a highly multimode guide.

The characteristic equation which determines the eigenvalues α is obtained by requiring H_z to be continuous at $x = b$:

$$\sin\left[k\sqrt{n_0^2-\alpha^2}\,b + 2\phi(\alpha)\right] = 0 \tag{A.4}$$

The paraxial approximation to these modes ($\alpha \simeq n_0$) is found as in [10]

by reckoning $\phi(\alpha)$ to be small. From (A.2) and (A.4), we then obtain approximately

$$\sin\left[k\sqrt{n_o^2 - \alpha^2}\,b(1 + 2/V)\right] = 0$$

or

$$\alpha_m = \sqrt{n_o^2 - \frac{m^2\pi^2}{k^2b^2(1+2/V)^2}} \tag{A.5}$$

i.e., the propagation constants for a parallel-plate waveguide of slightly larger width $a = b(1 + 2/V)$. The corresponding field within the slab is, from (A.1),

$$e^{-ik\alpha_m z} A \sin\left[k\sqrt{n_o^2 - \alpha^2}\,(x + b/V)\right] \qquad 0 \le x \le b \tag{A.6}$$

Here we have

$$\alpha_m = n_o - \frac{m^2\pi^2}{2n_o k^2 b^2 (1+2/V)^2} + O\left[\frac{m^4\pi^4}{k^2b^2V^3(1+2/V)^5}\right] \tag{A.7}$$
$$O\left[\frac{m^4\pi^4}{k^4b^4(1+2/V)^4}\right]$$

For most optical waveguides the first error term is likely to be the larger, but in any case we require

$$k^2b^2V^3 \gg 1 \qquad \text{and} \qquad k^4b^4 \gg 1$$

APPENDIX B

PROPERTIES OF $\vartheta_3(z|\tau)$

In this Appendix, we derive a number of useful properties of the theta-function $\vartheta_3(z|\tau)$, defined by

$$\vartheta_3(z|\tau) = \sum_{m=-\infty}^{\infty} e^{m^2\pi i\tau + 2miz} \tag{B.1}$$

where, for our purposes, z is an arbitrary complex number, while τ lies in the upper half-plane $\mathrm{Im}(\tau) \geq 0$. If τ lies on the real axis, we likewise require that z be real, and in this case $\vartheta_3(z|\tau)$ must be treated as a generalized function.

From Whittaker and Watson [25], we can obtain a number of periodicity and parity relations:

$$\vartheta_3(z|\tau) = \vartheta_3(-z|\tau) \tag{B.2}$$

$$\vartheta_3(z|\tau+2n) = \vartheta_3(z|\tau) \tag{B.3}$$

$$\vartheta_3(z+n\pi|\tau) = \vartheta_3(z|\tau) \tag{B.4}$$

$$\vartheta_3(z+n\pi\tau|\tau) = e^{-\pi i n^2\tau - 2inz}\vartheta_3(z|\tau) \tag{B.5}$$

(B.3)–(B.5): $n = 0, \pm1, \pm2, \ldots$

All four relations are easy consequences of the definition (B.1). It is also interesting to note that ϑ_3 satisfies the parabolic equation

$$\frac{\pi i}{4}\,\frac{\partial^2\vartheta_3(z|\tau)}{\partial z^2} + \frac{\partial\vartheta_3}{\partial\tau} = 0 \tag{B.6}$$

which is obtained from the Helmholtz equation in the paraxial approximation, and is similarly easily verified (cf. eqn.(8)).

For real z, ϑ_3 at $\tau = 0$ (as a generalized function) can be evaluated as [24],[26]:

$$\vartheta_3(z|0) = \sum_{m=-\infty}^{\infty} e^{2miz} = \pi \sum_{n=-\infty}^{\infty} \delta(z - n\pi) \tag{B.7}$$

Another useful relation, which holds for general z and τ, is obtained from Jacobi's imaginary transformation [21]:

$$\vartheta_3(z|\tau) = \tau^{-\frac{1}{2}} e^{i\pi/4 + z^2/\pi i\tau} \vartheta_3\left(\frac{z}{\tau} \,\middle|\, -\frac{1}{\tau}\right) \tag{B.8}$$

This relation can be verified using the Poisson summation formula [24].

The identities which form the basis for the "image-splitting" properties of the theta -function can be deduced from a more general expression given by Krazer [27]. These relations, which might be referred to as modular relations, are

$$\vartheta_3(z|\tau) = \sum_{r=0}^{p-1} e^{\pi i r^2\tau + 2irz} \vartheta_3(p[z+\pi r\tau]|p^2\tau) \tag{B.9}$$

$$\vartheta_3(z|\tau) = \frac{1}{p} \sum_{r=0}^{p-1} \vartheta_3\left(\frac{z+\pi r}{p} \,\middle|\, \frac{\tau}{p^2}\right) \tag{B.10}$$

Equation (B.9) is verified by writing $m = p\ell + r$, $r = 0,1,\ldots,(p-1)$ in (B.1); (B.10) follows by substituting (B.1) into the right hand side. Actually (B.9) and (B.10) can also be derifed from each other using (B.8) as well.

An integral which the authors could not find in the literature is given below:

$$\int_{-\infty}^{\infty} e^{-ax^2+bx}\, \vartheta_3(x|\tau)dx = \sqrt{\frac{\pi}{a}}\, e^{b^2/4a}\, \vartheta_3\left(\frac{b}{2a}\,\middle|\,\tau+\frac{i}{\pi a}\right) \tag{B.11}$$

The derivation is straightforward, proceeding by integrating (B.1) term-by-term.

Finally, we note that

$$\vartheta_3(iz|i\tau) = e^{z^2/\pi\tau} \sum_{m=-\infty}^{\infty} e^{-(z+m\pi\tau)^2/\pi\tau} \tag{B.12}$$

i.e., ϑ_3 can be related to a string of displaced Gaussian functions.

Figure Captions

Fig. 1: Parallel-plate waveguide.

Fig. 2: Imaging of a nonsymmetrical field distribution.

(a) Input function $E_y(x,0)$.

(b) $E_y(x,z_{21}) = E_y(a-x,0)$ (Inverted image).

(c) The three components of $E_y(x,z_{31})$;

$$E_y(x,z_{31}) = \frac{i}{\sqrt{3}} E_y(x,0) + \frac{e^{-i\pi/6}}{\sqrt{3}} \begin{cases} -E_y(\frac{2a}{3} - x, 0) ; & 0 \leq x \leq \frac{2a}{3} \\ E_y(x - \frac{2a}{3}, 0) ; & \frac{2a}{3} \leq x \leq a \end{cases}$$

$$+ \frac{e^{-i\pi/6}}{\sqrt{3}} \begin{cases} E_y(x + \frac{2a}{3}, 0); & 0 \leq x \leq \frac{a}{3} \\ -E_y(\frac{4a}{3} - x, 0) ; & \frac{a}{3} \leq x \leq a \end{cases}$$

(d) The two components of $E_y(x,z_{41})$;

$$E_y(x,z_{41}) = [e^{i\pi/4} E_y(x,0) + e^{3\pi i/4} E_y(a-x,0)]/\sqrt{2}.$$

Fig. 3: Imaging of a symmetric field distribution.

(a) $|E_y(x,0)| = |E_y(x,z_{21})| = |E_y(x,z_{41})| = |E_y(x,z_{81})|$.

(b) The three components of $E_y(x,z_{31})$.

Fig. 4: Overlapping of original and image beams in overmoded waveguide.

Fig. 5: Evaluation of power distribution of Gaussian beam over 1/8-cycle: $ka = 973.39$; $kw_o = 110.3$. (a) $z/z_{11} = 0$; (b) 3/512; (c) 8/512; (d) 13/512; (e) 16/512; (f) 22/512; (g) 28/512; (h) 32/512; (i) 55/512; (j) 64/512.

Fig. 6: Exact and approximate power patterns at large axial distance; $ka = 1538.23$; $kw_o = 174.3$; $z/z_{11} = 250.119$.

Fig. A.1: Dielectric slab waveguide

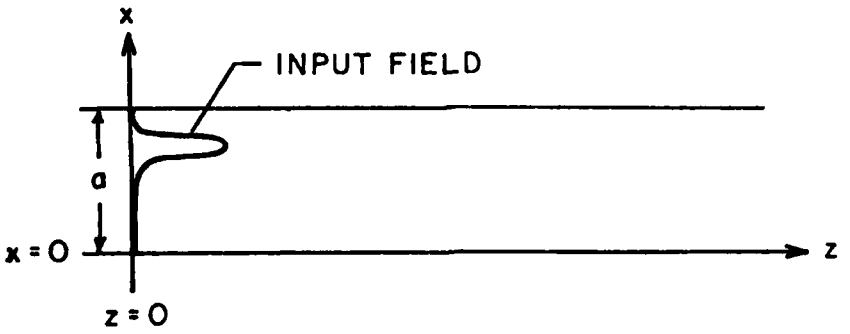

Figure 1

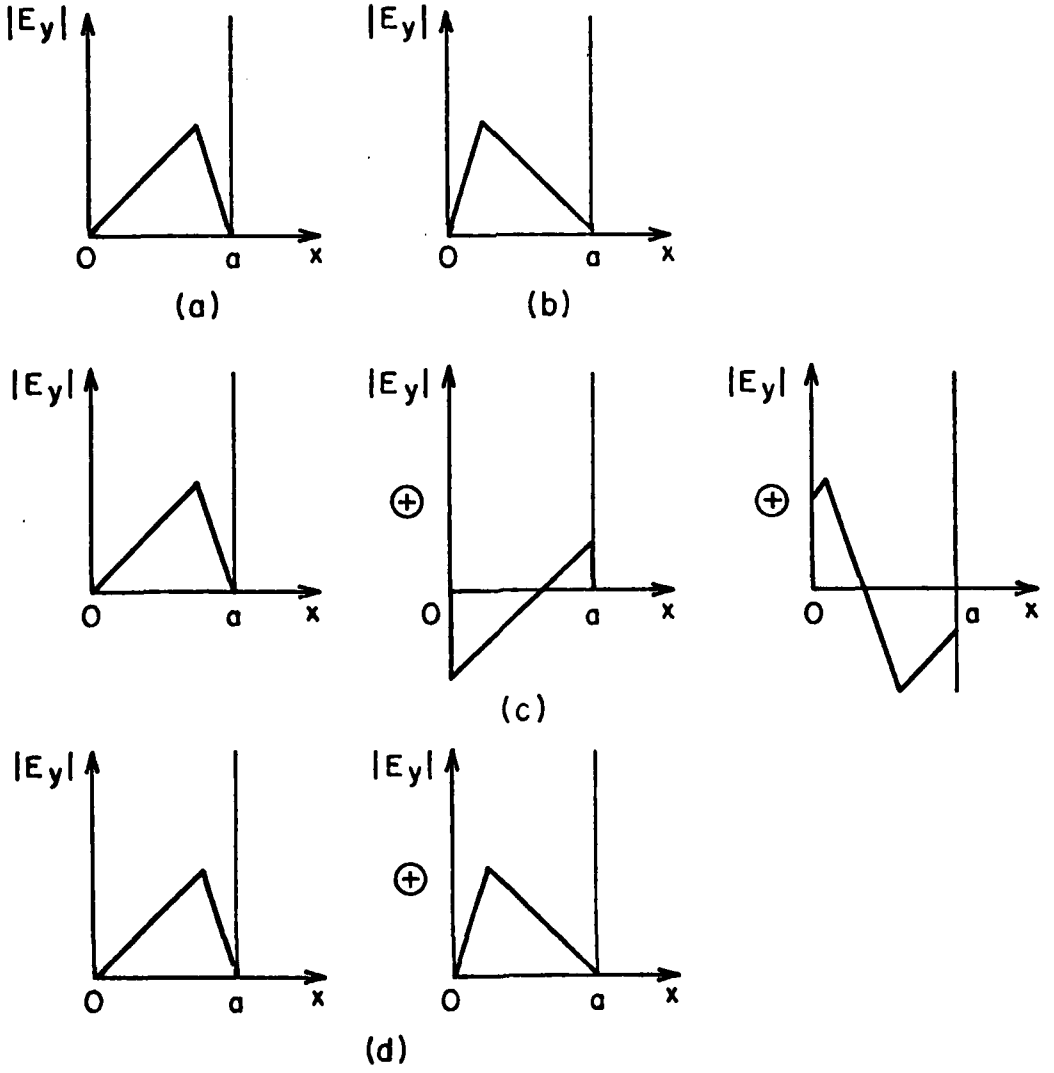

Figure 2

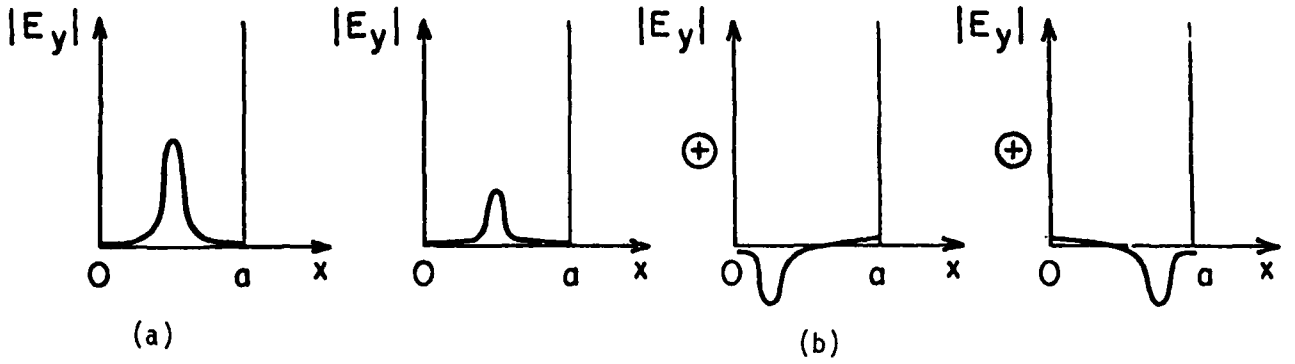

Figure 3

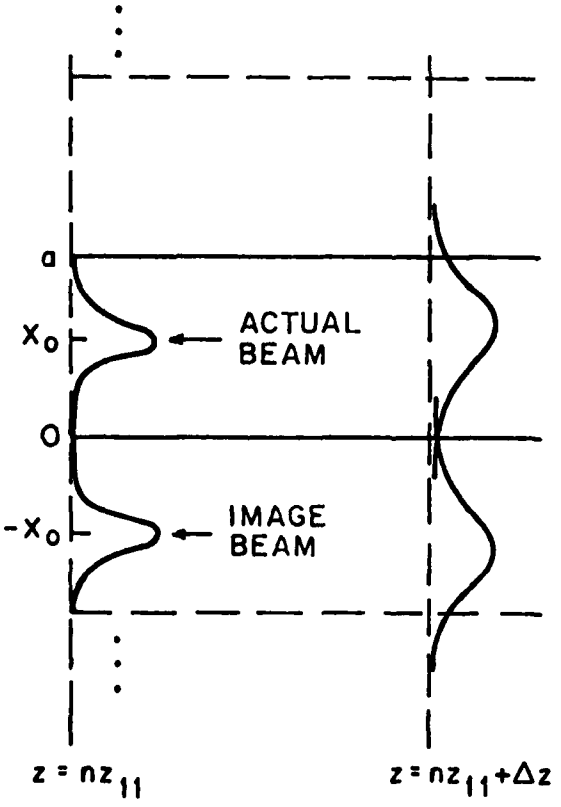

Figure 4

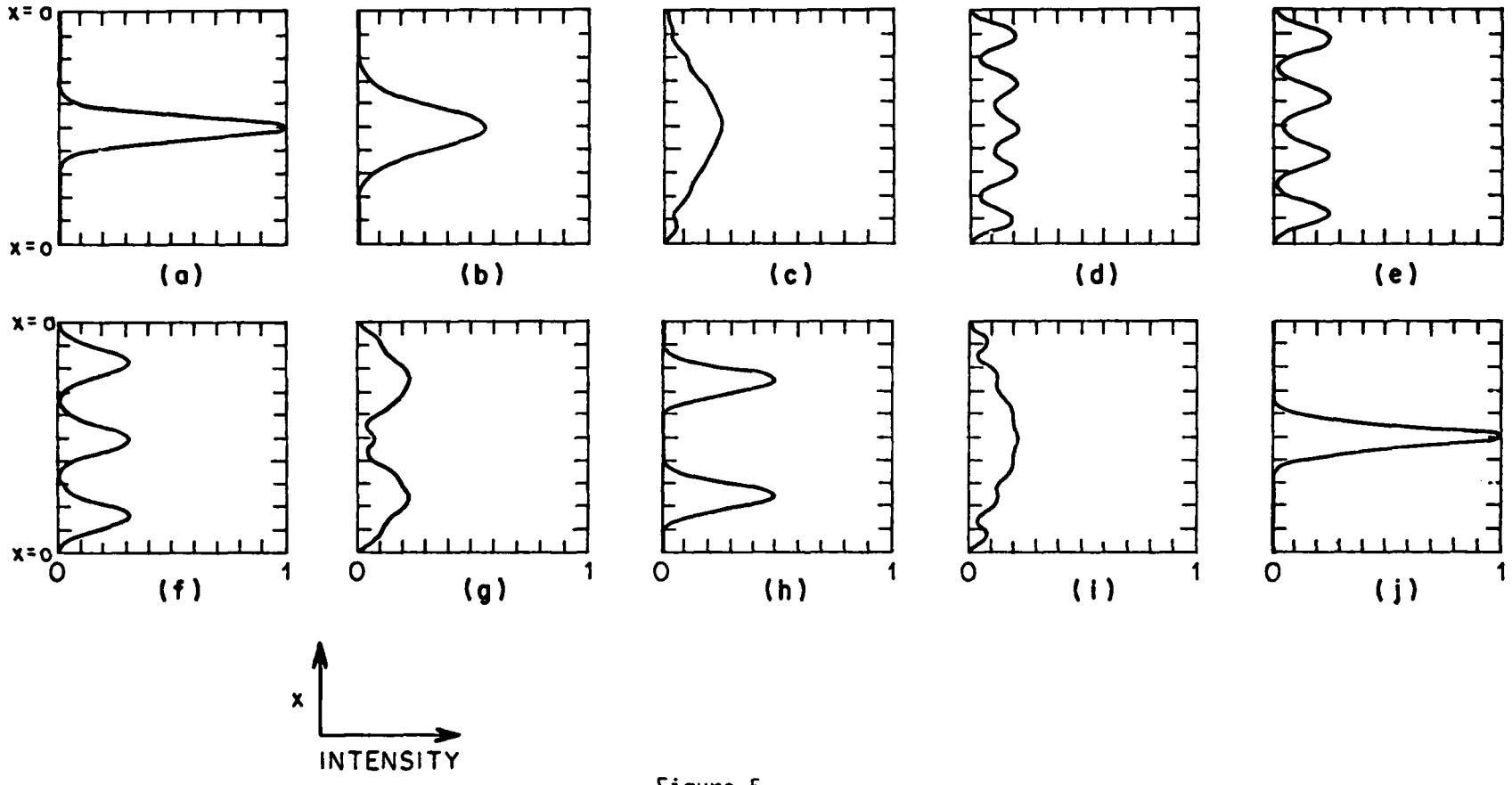

Figure 5

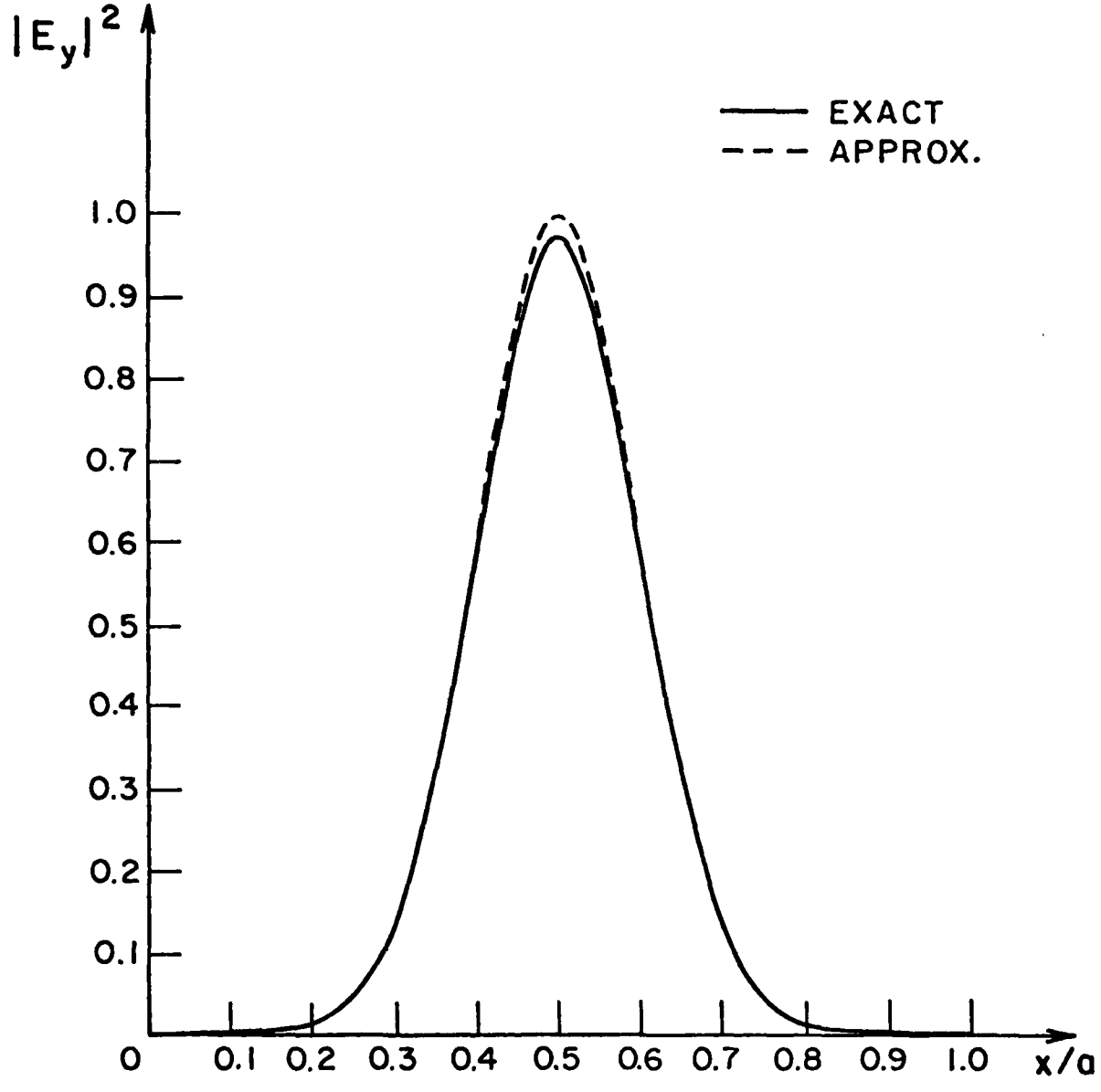
$|E_y|^2$
EXACT
APPROX.
1.0
0.9
0.8
0.7
0.6
0.5
0.4
0.3
0.2
0.1
0
0.1
0.2
0.3
0.4
0.5
0.6
0.7
0.8
0.9
1.0
x/a

Figure 6

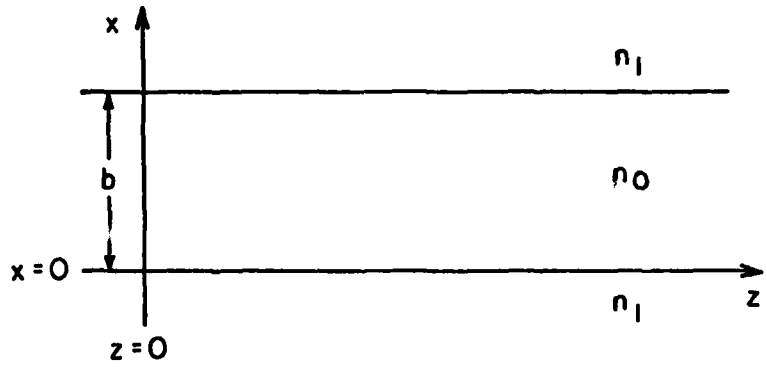

Figure A.1